We are IntechOpen, the world's leading publisher of Open Access books

Built by scientists, for scientists

6,900
Open access books available

185,000
International authors and editors

200M
Downloads

Our authors are among the

154
Countries delivered to

TOP 1%
most cited scientists

12.2%
Contributors from top 500 universities

CLARIVATE ANALYTICS

BOOK CITATION INDEX

INDEXED

WEB OF SCIENCE™

Selection of our books indexed in the Book Citation Index
in Web of Science™ Core Collection (BKCI)

Interested in publishing with us?
Contact book.department@intechopen.com

Numbers displayed above are based on latest data collected.
For more information visit www.intechopen.com

Chapter

Experimental Study of CO_2 Plasticization in Polysulfone Membrane for Biogas Processing

Serene Sow Mun Lock, Kok Keong Lau, Azmi Mohd Shariff, Yin Fong Yeong and Norwahyu Jusoh

Abstract

Polymeric membranes have emerged for biogas processing to remove CO_2 from CH_4. Nonetheless, it is also acknowledged that polymeric membranes have the tendency to sorb highly condensable CO_2, which consequently swells the polymeric matrix, typically at operating condition higher than the plasticization pressure. The swelling increases void spaces for transport of gas penetrants, which results in an increment in permeability of all gas components at the cost of substantial decrease in membrane selectivity. Despite observations of the end results of plasticization, it is found that many transport property studies include only permeability measurements near ambient conditions. Complementary information on the individual contributions of the sorption and diffusion coefficients to the overall performance typically at non-ambient operating conditions is rarely reported. Therefore, in present study, experimental study has been conducted to fabricate polysulfone (PSF) film. Validity of the developed polysulfone membrane has been verified through characterization and validated with gas transport behavior of published results. Subsequently, transport properties of CO_2 though the PSF membrane at varying operating temperatures has been elucidated. The dual mode sorption and partial immobilization models have been employed to quantify the gas transport properties of noncondensable CH_4 and condensable CO_2 through PSF membrane.

Keywords: membrane, plasticization, solubility, diffusivity, permeability

1. Introduction

The ever-growing worldwide energy demand has directed the attention of government agencies and energy companies towards uncovering renewable energy over recent years as an alternative to achieve sustainable global energy policy [1]. The effort is done to circumvent the volatility of fuel price in the petrochemical market while meeting expanding user demand [2]. Biogas produced from microbial digestion of waste is found to contain high concentration of methane (CH_4), which can be utilized for combustion process to circumvent usage of fossil fuels while meeting energy demand. Nonetheless, biogas also contains a huge amount of side products, typically carbon dioxide (CO_2), whereby the amount can reach as high as 50% [1].

It is highly desirable to remove the CO_2 contaminants from CH_4 since the unequivocal symptoms of climate change have urged continuous pressure on oil and gas companies to adopt practices that reduce carbon footprint to mitigate the effect of greenhouse gases global warming [3]. In addition to minimization of the environment pollution, the undesired CO_2 must be removed in order to increase the heating value of biogas since the abundant impurities constitute to no heating value [4]. The removal of CO_2 in the biogas also prevents corrosion of pipelines and process equipments that are of great importance to curb gas leakage along the transportation process since the leakage can contribute to public hazards [5]. It has been proposed that the produced biogas requires processing to contain a minimal of 95% CH_4 in order to be economically viable [1].

Polymeric membrane applied in gas separation is an alternative that has gained attention in industrial scale application in comparison to conventional technologies (e.g. distillation and absorption) over recent years. The advantages associated to polymeric membrane include taking up a considerably confined space, merely involves physical separation that is free from chemical reaction for consideration of process safety, lower energy consumption and smaller operating cost requirement [6, 7]. Polymeric membrane has been utilized exceptionally in application of CO_2 removal from CH_4 for processing of biogas. However, a problem that hinders further expansion of the usage of polymeric membranes in such application has emerged due to CO_2 induced plasticization.

During CO_2 plasticization, sorption of condensable gas penetrants in the membrane matrix interacts with functional group of the pristine polymeric chain. The interaction contributes to ease of mobility of polymeric chains, which consequently increases the void channels in the membrane [8]. Schematic representation of the plasticization phenomena that increases free volume of the polymeric glassy membrane is provided in **Figure 1** [9].

As a result, plasticization increases void channels that form passage for gas permeation of all gas species [10]. Nonetheless, when empty spaces increase, the sieving capability of the polymeric membrane also reduces simultaneously. This causes reduction in the membrane selectivity $\left(\propto_{A/B} = P_A/P_B \right)$ as an ultimate result. Therefore, it is vital to understand CO_2 plasticization in polymeric membranes since it is highly possible to cause undesirable product lost that decreases profitability of the biogas processing plant.

The observation of CO_2 plasticization in glassy polymeric membranes has been well addressed with a long history. Wessling et al. conducted experiments comparing the kinetics of mass uptake (sorption) and the volume increase (dilation) due to sorption to give a deeper understanding of the plasticizing effect of CO_2 in commercial 6FDA membrane [11]. Houde et al. employed the wide angle X-ray diffraction (WAXD) to investigate the mechanism of plasticization in various glassy polymers [12]. Bos et al. reported CO_2 plasticization phenomena, which includes
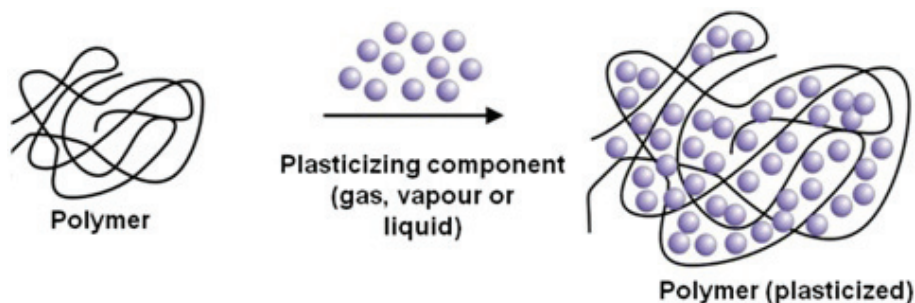

Figure 1.
Plasticization phenomena resulting in facilitated polymer mobility and increased free volume in the polymer, adapted from Kikic et al. [9].

that of plasticization pressure and amount of CO_2 that invoke plasticization, in different glassy polymer classes through measurement of gas permeation and sorption [10]. Kapantaidakis et al. demonstrated accelerated CO_2 plasticization effect in ultrathin polymer structures by measuring gas permeance at increasing operating pressures [13]. Horn and Paul [14] studied the CO_2 plasticization (reversible) and conditioning (non-reversible) effects in thin and thick glassy polymeric membranes to reaffirm conclusion by Kapantaidakis et al. [14]. Tiwari et al. extended the study by Horn and Paul [14] to high free volume glassy perfluoropolymers through evaluation of CO_2 permeability and ellipsometry measurement [15]. Reviews of study related to CO_2 plasticization in different membranes have been provided in works by Suleman et al. [16].

From previous works, it is found that many transport property studies devoted to plasticization include only study of membrane morphology and permeability measurements near ambient conditions. Complementary information on the individual contributions of the sorption and diffusion coefficients to the overall performance at non-ambient and elevated temperatures is rarely reported. Most of the laboratory data have been limited to study of gas transport characteristic within polymeric membrane at ambient operating temperatures (25–35°C). This is because it appears to be not convenient and time consuming to control the operating conditions at different ranges.

Hence, the objective of present study is to study the effect of CO_2 to plasticization of Polysulfone membrane at varying operating conditions. PSF have the most advantages among all polymeric membranes since it easily forms thin film on membrane support surfaces, while demonstrating behaviors such as chemical inertness, good mechanical strength and stable property, which have encouraged their usage in biogas processing. Bos et al. reported a plasticization pressure of 34 bar at 23°C [10] for polysulfone. Nonetheless, the collected data is limited and not extended to elevated pressure, as well as other operating temperatures. In typical biogas processing, the entering gas are in the range of 35–55°C in order to suit the temperature for membrane separation [17]. In our recent work, we studied the interaction of CO_2 with polysulfone membranes at varying operating temperatures and CO_2 concentrations through employment of atomistic simulation technique and concluded that lower operating temperature constituted to more apparent plasticization effect to membrane morphology [18]. Nonetheless, the study has not been extended to study of gas transport property.

Therefore, this work aims to assemble a sequence of experimental procedure to study gas transport property, which includes solubility, diffusivity and permeability, during plasticization at varying operating temperatures. In an overall, firstly PSF membrane has been fabricated through in-house experimental procedure. Then, the PSF membrane has been analyzed through characterization in order to evaluate applicability of developed membrane. Subsequently, the solubility and permeability of noncondensable methane at varying operating temperatures have been measured and validated with published experimental data to determine applicability of the experimental setup. Then, the gas transport property of condensable CO_2 at different operating temperatures has been elucidated to study CO_2 plasticization effect in membrane. Finally, empirical models have been used to quantify gas transport behavior of the gases.

2. Methodology

This section discusses the methodology that has been adapted in current work. The overall workflow is presented in **Figure 2**.
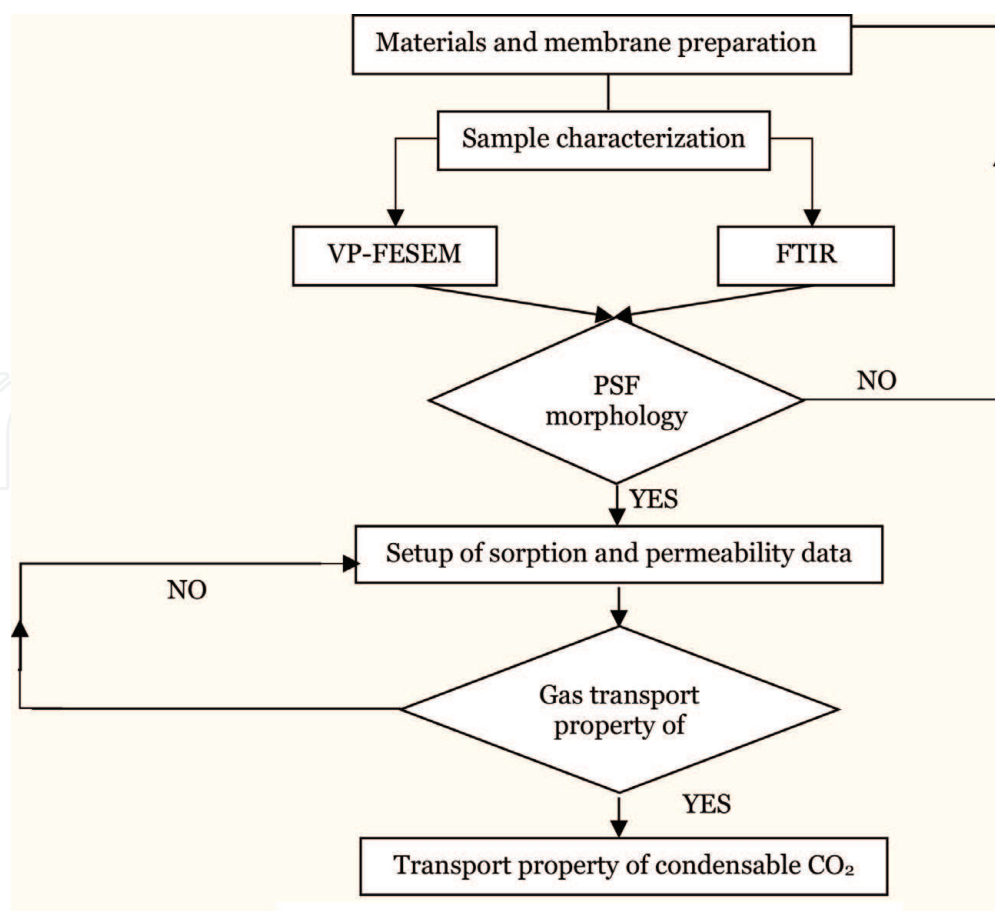
Figure 2.
Process diagram of overall workflow.

This section describes the materials and fabrication methodology to prepare the PSF membrane as well as analysis methodology to validate the developed membrane. In addition, the pressure decay and constant-pressure variable volume methodology for measurement of gas penetrants solubility and permeability have been elaborated.

2.1 Materials and membrane fabrication

The polysulfone (PSF) dense film was prepared via solution casting method using N-Methyl-2-pyyrolidone (NMP) as solvent [19, 20] with a composition of 25 wt% PSF. The PSF was manufactured and supplied in pellet form by Aldrich (MW ~35,000 by light scattering) while NMP from Merck (analytical grade) was used as received. Flow diagram characterizing the chronological procedure for fabrication of PSF dense membrane is depicted in **Figure 3**.

In the beginning, the PSF pellets were dehydrated overnight to get rid of unwanted water content by heating it in a vacuum oven. Subsequently, the amount of dried PSF pellets and filtered NMP solvent was measured prior to mixing them together for 24 hours. When approaching the end of the mixing process, a clear homogenous solution was observed.

Then, an ultrasonication water bath has been employed to desonicate the mixture with a total duration of 4 h before leaving it for 24 h free standing degas. This is aimed to remove any bubbles formed during the mixing protocol while enhancing its homogeneity. The casting solution was then poured into a leveled and clean glass Petri dish, which was covered with aluminum foil to reduce its evaporation rate.
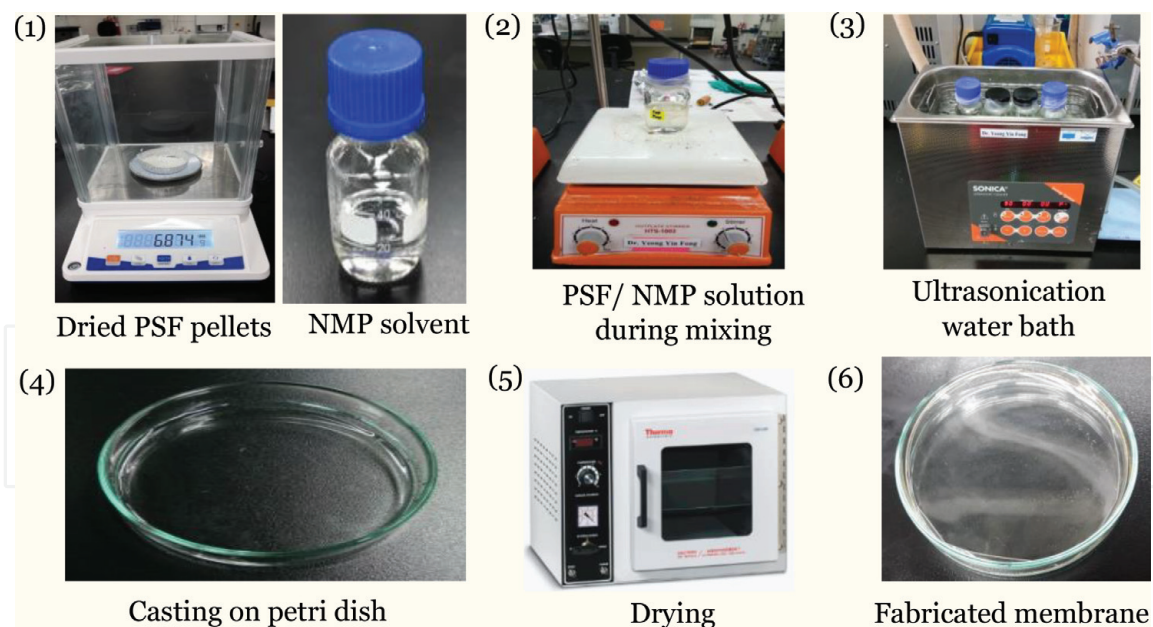
Figure 3.
Flow diagram of procedure for preparation of PSF membrane.

Subsequently, the membranes were subjected to vacuum drying at a heating rate of 20°C/h from 40 to 180°C followed by annealing at 180°C for 24 h. This is to prevent formation of defects in the membrane due to fast evaporation of the solvent. Finally, the PSF membrane film was carefully peeled off from the Petri dish once the cast solution was completely dried.

2.2 Sample characterization

In this section, the characterization analysis that has been used to investigate morphology of the prepared membrane has been discussed. The analysis is crucial to evaluate that the fabricated PSF membrane is dense and defect free. At the same time, it is aimed to ensure that all undesirable solvents that can potentially affect membrane characteristic have been removed accordingly. This is to confirm its applicability prior to measurement of gas solubility and permeability behavior in subsequent sections.

2.2.1 Variable pressure field emission scanning Electron microscope

The variable pressure field emission scanning electron microscope (VP-FESEM, Zeiss Supra 55 VP) was employed to evaluate membrane morphology of the fabricated PSF membrane. Cross sectional side of the membranes were prepared for VP-FESEM analysis via immersion in liquid nitrogen before fracturing the film in order to prevent morphology distortion. All the membrane samples were subsequently sputter coated with platinum using Quorum Q150R S coater prior to imaging. Membrane samples were observed using VP-FESEM with magnification at 500.

2.2.2 Fourier transform infrared spectrometer

Fourier transform infrared spectrometer (FTIR, Perkin Elmer Spectrum One) was operated under transmission with 50 scans in the wavelength range of 450–4000 cm^{-1} to determine IR spectra of the fabricated PSF membrane.

2.3 Solubility measurement (pressure decay methodology)

The principle is based on a dual-chamber pressure decay setup, which has been demonstrated in detailed elsewhere [21]. In this approach, the quantity of gas originally introduced to a sorption system and equilibrated quantity of gas left behind after sorption into a polymer located within the sorption system are determined. This requires measurement in the decline of pressure after sorption of gas into a polymer under study, the temperature of gas, and volume of the system in which the experiment takes place. By measuring the aforementioned variables, the initial and final number of gases existing in the sorption system can be determined directly.

The concentration of gas molecule, x, sorbed within the polymer membrane at any operating temperature has been obtained through Eq. (1), where 22,414 cm^3/mol corresponds to a simple numerical conversion factor and V_p (cm^3) is volume of the polymer sample in the membrane chamber, which has been determined through the conventional fluid displacement method.

$$x = n_p \left(\frac{22414}{V_p} \right) \qquad (1)$$

In this study, in order to invoke sorption of polymeric membranes at varying operating temperatures, a constant temperature water bath has been employed. In this context, temperature of the system is consistently controlled at the designated value by submerging the sorption cell within the temperature regulated water bath. Operating temperature is increased gradually from 35 to 55°C with an interval of 10°C for each incremental step. As for pressure increment, it has been continually increased from 5 to 50 bars with an interval of 5 bars to determine sorption isotherm of gases. CH_4 gas has been introduced to the sorption cell first prior to CO_2 since condensable gases can potentially cause irreversible plasticization and swelling effect to the membrane morphology that affects its sorption capability as an end result.

2.4 Permeation measurement

This section describes the experimental setup for gas permeation testing across the PSF membrane. The apparatus adopted a constant-pressure variable volume system to measure gas permeability by measuring the permeate flow rate at atmospheric downstream pressure using a bubble flow meter. Schematic diagram for gas permeation measurement has been provided in **Figure 4**.

The system consists of a feed inlet point, a pressure regulation system and a mass flow controller. The amount of gas from feed inlet point was controlled using a mass flow controller. The permeation apparatus is developed for high pressure testing devoted to CO_2 and CH_4. For high pressure applications, all fittings and valves were supplied by Swagelok with pressure-rating > 70 bar while all sensors are capable to read a maximum pressure of 100 bars. In addition, operating temperature of the membrane has been controlled at constant and designated value by regulating oven temperature. Before conducting experiment, the system has been evacuated with a vacuum pump overnight to eliminate any gas or vapors in the system. Leak tests have been performed after degassing process to ensure that the equipment is safe before experiment proceeded.

For polymer structure, it is important to heat it ~10°C above its glass transition temperature, T_g, in the absence of any mechanical stress to erase all previous thermal history as well as to relax any molecular orientation captured during film formation [22]. The thermal history removal protocol has been adapted from
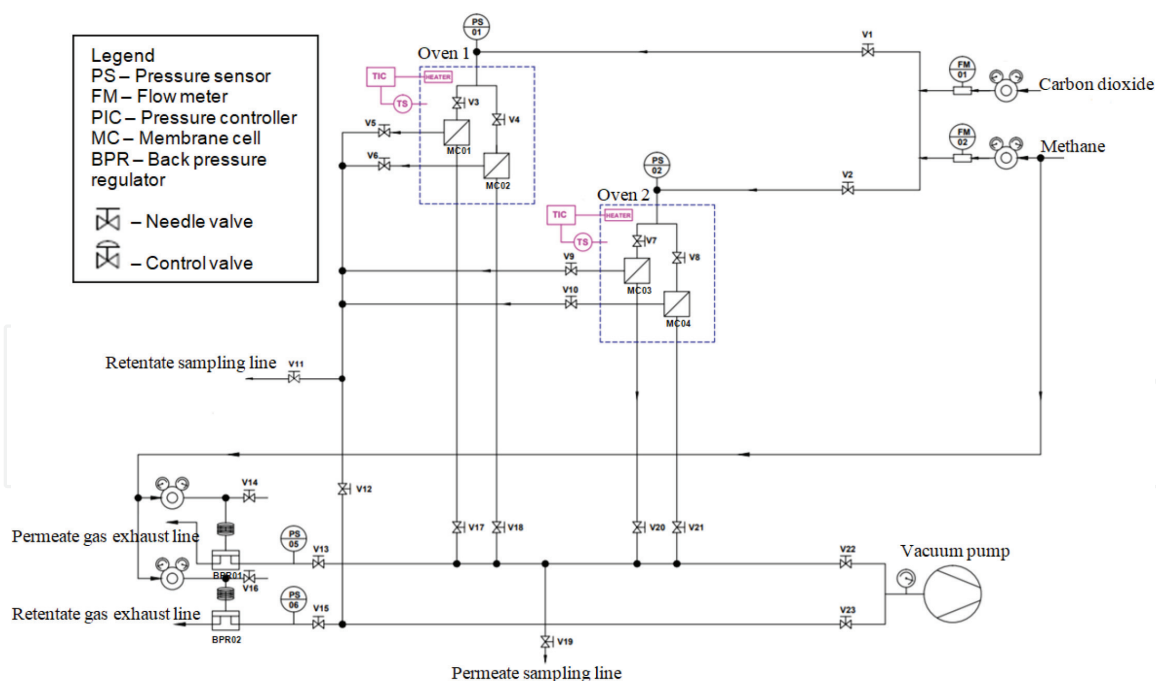
Figure 4.
Parallel membrane cell for reproducibility of gas permeation.

Huang et al. work [22]. The procedure has been conducted in the vacuum oven for 30 min to prevent any oxidation since equilibration at the rubbery state should be tentatively achieved over this time span based on Struik's report [23]. After heating, the polymer membrane has been immediately removed from the vacuum oven and has been quenched to ambient temperature, while preparing the membrane for permeation test.

For the separation process, the membrane sample of 3.14 cm^2 effective area has been mounted in a membrane test cell to study the separation efficiency at various operating conditions. The membrane area has been constituted by cautiously locating the membrane films on aluminum tape over a circle hole with a diameter of 1 cm while avoiding any folding that destroys the membrane surface. Finally, a second piece of aluminum tape and Whatman® Anodisc filter has been adhered to the underside of the membrane for mechanical support to withstand a wide range of operating pressure.

The process of mounting the membrane within the test cell has been conducted within 15 min before bringing the polymer membrane to the desired operating temperature, which are 35, 45 and 55°C respectively. The pressure has been increased gradually from atmospheric condition to a maximum of 50 bars with an increment step of 5 bars. Upstream gas at required operating pressure, temperature and flow rate has been introduced into the membrane for permeation test. Volumetric permeation rates in the permeate stream has been determined with a soap bubble flow meter. Lastly, the entire system should be evacuated to fully degas the system before proceeding to other experiment.

At least three measurements were performed to evaluate the flowrate and composition during membrane separation process. Since the current study addresses high pressure conditions, non-ideal gas conditions should be considered. The driving force for this case is described as the distinction in fugacity from the high to low end across the membrane. A nonideal equation of state has been employed to compute fugacity of CO_2 and CH_4 on the feed side. On the other hand, since the permeate pressure is remained at atmospheric condition, the nonideality associated to real gas behavior can be disregarded. The permeability of gas component i (barrer), P_i, is calculated based on Eq. (2).

$$P_i = \frac{t V_P}{A_m \left(f_h - f_l \right)} \qquad (2)$$

In Eq. (2), V_P is the permeate flow rate (cm^3 (STP)/s), t is the thickness of membrane (cm), A_m is the membrane area (cm^2), f_h and f_l are the fugacities in feed side and permeate side respectively (cmHg), subscript i denotes CO_2 or CH_4. The permeability of the membrane is expressed in the unit of Barrer (1 Barrer = 1×10^{-10} cm^3 (STP) cm/s cm^2 cmHg).

3. Results and discussion

In this part, the results pertaining to experimental section from the fabricated PSF polymeric membrane, gas transport properties of incondensable CH_4 and condensable CO_2 within the PSF membrane and empirical model to quantify the permeation behavior have been discussed.

3.1 Membrane morphology

To understand the membrane morphology, several characterization methodologies have been conducted to analyze the fabricated membrane, which comprised those of VP-FESEM and FITR, as discussed in the subsections.

3.1.1 VP-FESEM

The structure of dense PSF membrane at a magnification of 500 is depicted in **Figure 5**.

The PSF membrane is consisted of a dense, nonporous and single polymer layer that is homogenous in all directions. The thickness of the membrane is ∼78 μm. The smooth membrane configuration without defects ensures its applicability for solubility and gas permeation measurement in subsequent section.
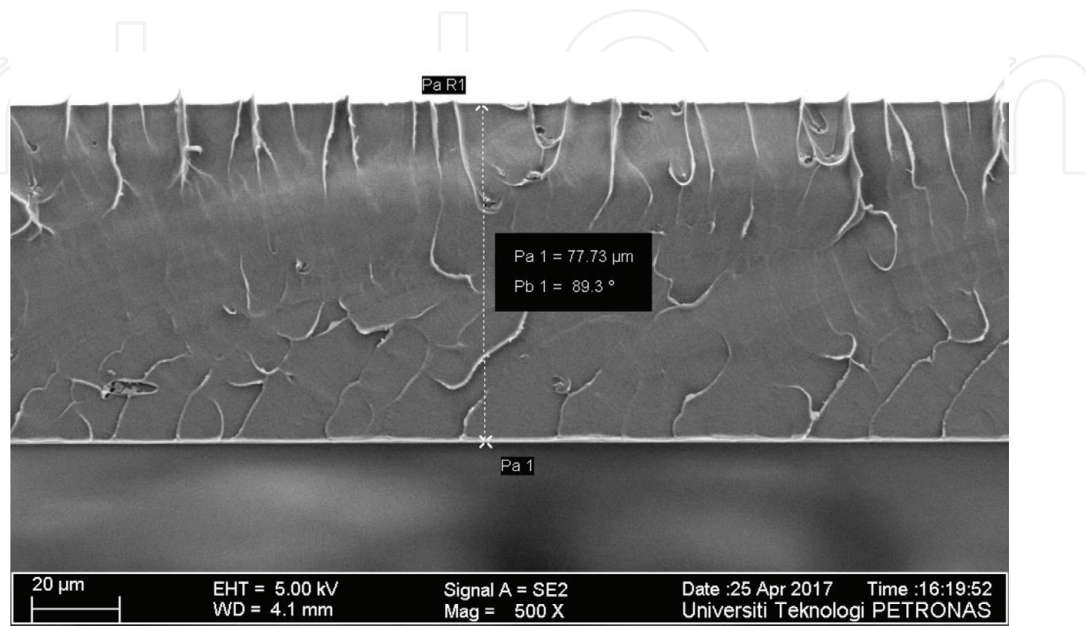

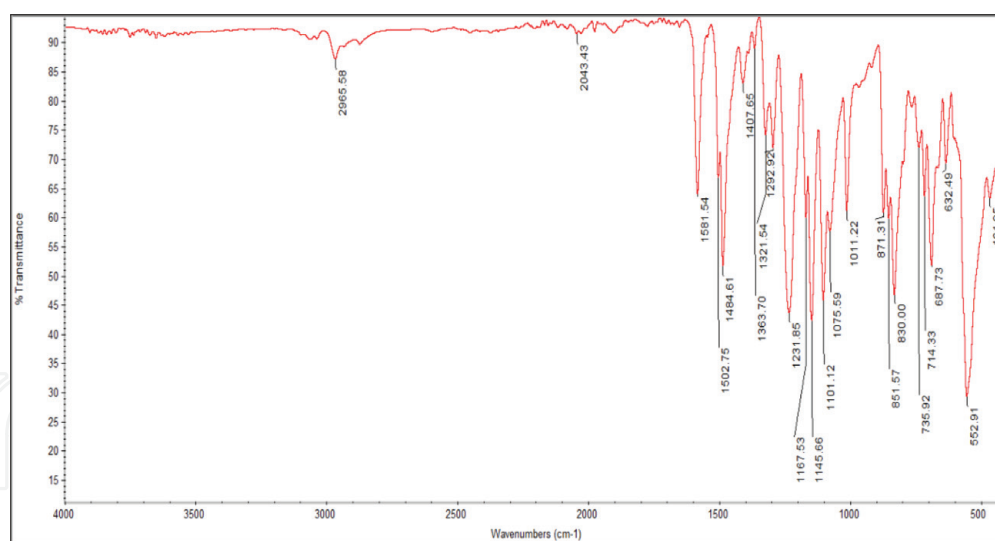**Figure 5.**
Cross sectional of PSF dense membrane.

Figure 6.
FTIR spectrum of synthesized PSF membrane.

3.1.2 FTIR

FTIR is the most effective alternative to elucidate the functional group of membrane. **Figure 6** depicts the IR spectrum of the PSF polymeric membrane obtained in present work.

For PSF membrane, the peak at 2965.58 cm^{-1} correspond to stretching vibration of asymmetric and symmetric C-H bond. On the other hand, the peaks at 1581.54 and 1484.61 cm^{-1} represent the C=C bond in the PSF repeat chain. The IR spectra peak observed at 1407.65 and 1363.70 cm^{-1} correspond to the asymmetric and symmetric C-H bending deformation of methyl group. Amine stretching is depicted at 1101.12 cm^{-1}, while phenyl ring substitution band is noticed at 851.57, 830.00, 714.33 and 687.73 cm^{-1}. IR spectrum noticeable at 1231.85 cm^{-1} represents the presence of asymmetric C-O-C stretching by aryl ether group. The peaks at 1167.53 and 1101.12 cm^{-1} are assigned to asymmetric and symmetric O=S=O stretching of sulfonate group. In addition, the peak at 1407.65 cm^{-1} has been attributed to stretching vibration of aromatics in PSF. All the functional groups are consistent to those observed in the repeat unit of Polysulfone [18]. The good accordance demonstrates the validity of the synthesized PSF membrane and elimination of any impurities/solvent that can potentially affect the membrane separation performance.

3.2 Validation with transport properties of methane

To validate applicability of the sorption laboratory setup, gas methane has been introduced to the PSF membrane with operating pressure at an incremental step, to acquire the sorption behavior of CH$_4$ in PSF membrane, as shown in **Figure 7**. Experimental data by Sada et al. that studied the effect of operating temperature to the solubility of CH$_4$ within PSF has also been provided as Ref. [24]. The sorption experimental data obtained from current work exhibits close agreement with published results by Sada et al. [24]. The good compliance suggests that the fabricated PSF polymeric membrane and experimental setup are of adequate soundness to produce defects and error free experimental results.

From **Figure 7**, it is shown that the concentration of CH$_4$ being sorbed into the polymeric membrane is enhanced when operating pressure increases at all operating temperature. The increment in CH$_4$ concentration can be explained through greater driving force that advances the sorption of gas molecules within the free
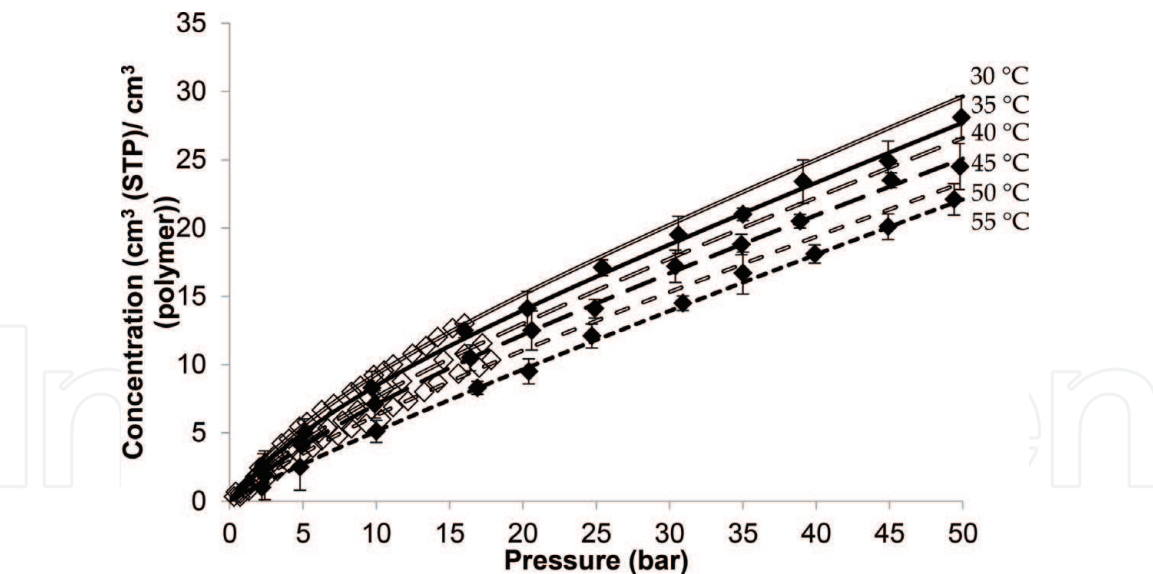
Figure 7.
CH_4 sorption isotherm for polysulfone. [♦ In-house collected sorption data ◊ Sorption data by Sada et al. [24].
*Close line - Prediction of dual mode sorption model by Eq. (3) with parameters in **Table 1** for in-house*
collected sorption data Open line - Prediction of dual mode sorption model by Eq. (3) with parameters in
***Table 1** for sorption data by Sada et al. [24]. (———— 30/35°C, — — — ·40/45°C, - - - - - ·50/55°C)].*

spaces of polymeric membrane matrix. The sorption of CH_4 gas molecules is found to be decreasing when operating temperature is increased [18]. The decrement is intuitively reasonable since gas molecules have higher affinity to remain in the gaseous state than rather being sorbed into the membrane at higher operating temperature. In addition, the sorption isotherm of CH_4 is found to exhibit good correlation to the dual mode sorption model as depicted in Eq. (3).

$$C_i = C_{Di} + C_{Hi} = k_{Di}f_i + \frac{C'_{Hi}b_if_i}{1 + b_if_i} \qquad (3)$$

The dual mode sorption model suggests that the total concentration of gas *i* in a polymer matrix is composed of two idealized molecular scale environment, in which C_i is the total concentration of gas in the polymer; C_{Di} is equilibrium population existing in the polymer matrix under the dissolved mode and is governed by Henry's Law equation, while C_{Hi} is the non-equilibrium population existing in excess within the hole-filling environment governed by Langmuir parameters [25–27]. Moreover, k_{Di} is the Henry's law coefficient that characterizes dissolution of a pure gas, *i*, in the polymer, b_i and C'_{Hi} is the Langmuir hole affinity parameter and the capacity parameter respectively, while f_i is fugacity of the gas system [26, 28]. The fitted dual mode sorption parameters are provided in **Table 1**, which has been summarized alongside the reported values by Sada et al. [24].

In has been demonstrated from **Table 1** that the parameters are in satisfactory agreement with one another, attributed to the small distinction of the solubility

Temperature (°C)	k_{Di} (cm³(STP) cm³⁻¹ bar¹)	b_i (bar⁻¹)	C'_{Hi} (cm³ (STP) cm³⁻¹)
35	0.4123 (0.4352 @ 30°C)[a]	0.1055 (0.1145 @ 30°C)[a]	8.45 (9.26 @ 30°C)[a]
45	0.3859 (0.4076 @ 40°C)[a]	0.0812 (0.0874 @ 40°C)[a]	7.21 (7.63 @ 40°C)[a]
55	0.3589 (0.3711 @ 50°C)[a]	0.0678 (0.0738 @ 50°C)[a]	5.34 (6.03 @ 50°C)[a]

[a]The number in bracket is the experimental value by Sada et al. [24].

Table 1.
Dual-mode sorption parameters for methane in polysulfone film as a function of operating temperature.

characteristics as a whole. The reported values are found to be consistently higher for lower operating temperature attained through higher sorption capacity as explained earlier. The good compliance with previous published literatures and fit to the commonly employed dual mode sorption model demonstrates that the dual mode sorption cell is of high accuracy for plasticization study in subsequent section.

Similarly, validity of the gas permeation cell has been investigated by comparing measured methane permeability data with published experimental results by Sada et al. [24], such as that shown in **Figure 8** whereby a close agreement has been obtained in between the two. Measured permeabilities for methane in polysulfone films are illustrated as a function of upstream gas pressure in **Figure 8**. At every temperature, the mean permeability coefficients were found to decrease with an increase in upstream pressure. Such pressure dependence seems to be characteristic of glassy polymers. The gas permeability is found to be consistently higher at greater operating temperature. The contributing factor is free volume within the structure of the polymer has increased as the temperature is further increased, while gaining additional energy to execute diffusional jump.

The permeability of gas through a glassy polymeric membrane is frequently characterized through the partial immobilization model [29], which has evolved from the dual mode sorption model in Eq. (3), such as that presented in Eq. (4).

$$P_i = k_{D,i} D_{0,i} \left[1 + \frac{F_i C'_{Hi} b_i}{1 + b_i f_i} \right] \qquad (4)$$

In Eq. (4), $k_{D,i}$, C'_{Hi} and b_i are parameters from dual mode sorption model, while $D_{0,i}$ and F_i represent the diffusion coefficient in the limit when concentration of the mobile gas $C_{M,i} \rightarrow 0$ and the ratio of the diffusivity through the microvoids to that through the polymeric matrix. The additional parameters in the model have been summarized in **Table 2**.

For these results, $D_{0,i}$ and F_i appear to be a function of temperature. It is found that $D_{0,i}$ increases with increment in temperature, which has been rationalized through the enhancement in diffusion energy. A small F_i value corresponds to a relatively low diffusivity through the Langmuir regions. At lower operating
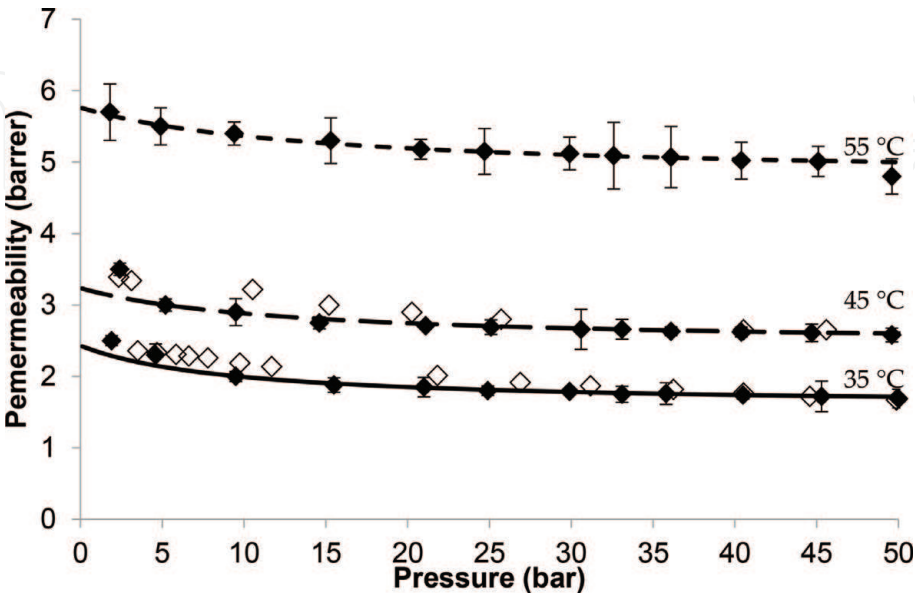

Figure 8.
*CH₄ gas permeability data for polysulfone. [♦ In-house permeability data ◊ Permeability data by Sada et al. [24]. Line - Prediction of partial immobilization model by Eq. (4) with parameters in **Table 2** for in-house collected permeability (———35°C, — — — ·45°C, - - - - - ·55°C)].*

Temperature (°C)	$D_{0,i}$ (cm²/s)	F_i
35	2.87×10^{-8}	0.607
45	4.75×10^{-8}	0.554
55	9.98×10^{-8}	0.507

Table 2.
Partial immobilization parameters for methane in polysulfone film, model adapted from Scholes et al. [29].

temperature, the Langmuir microvoids exist in a large number with greater sizes [29]. Therefore, gas molecules have a higher tendency to be transported through the Langmuir regions with lower resistance. When operating temperature is further increased, there is a reduction in the number and size of Langmuir microvoids, which consequently restraints the transport in such region. Therefore, there is a shift from dominancy of Langmuir to Henry's region with increment in operating temperature, which contributes to a smaller F_i value. In a similar manner, the satisfactory compliance with Sada et al. published literatures and fit to the commonly employed partial immobilization model demonstrates that the permeation cell rig is of high accuracy for measurement of CO_2 plasticization study in next section.

3.3. CO_2 plasticization in PSF membranes

CO_2 sorption in PSF membrane has been measured with increment in operating pressure at varying operating temperatures, such as that provided in **Figure 9**.
Published literature data by Sada et al. for solubility of CO_2 within PSF has also been provided [24]. In an overall, it is depicted that the collected sorption data of present study is not substantially different from the reported values by Sada et al. [24]. The sorption data of present work is consistently higher than that reported by Sada et al. at different operating temperatures, which can be deduced via the difference in source of polysulfone to prepare the membrane samples. The sorption data also demonstrates a good agreement with the dual mode sorption model, with close compliance with that reported by Sada et al. [24], such as that summarized in **Table 3**.
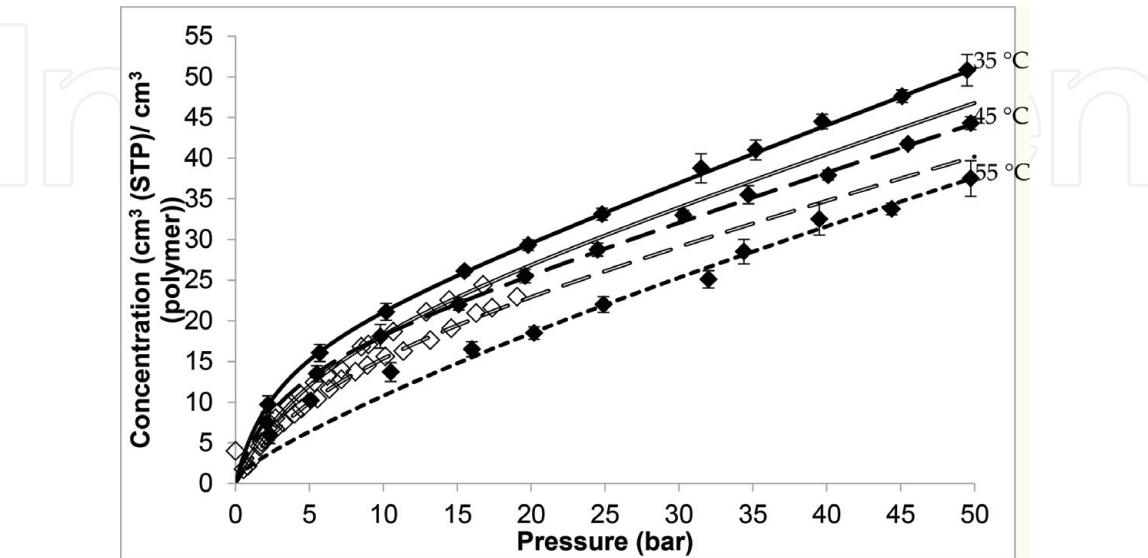

Figure 9.
*CO_2 sorption isotherm for polysulfone. [♦ In-house collected sorption data ◇ Sorption data by Sada et al. [24]. Close line - Prediction of dual mode sorption model by Eq. (3) with parameters in **Table 3** for in-house collected sorption data Open line - Prediction of dual mode sorption model by Eq. (3) with parameters in **Table 3** for sorption data by Sada et al. [24] (——— 35°C, — — — 45°C, - - - - - 55°C)].*

Temperature (°C)	k_{Di} (cm³(STP) cm³⁻¹ bar¹)	b_i (bar⁻¹)	C'_{Hi} (cm³ (STP) cm³⁻¹)
35	0.6748 (0.5872)[b]	0.3678 (0.1757)[b]	18.20 (19.40)[b]
45	0.5840 (0.5014)[b]	0.3415 (0.1530)[b]	15.93 (17.1)[b]
55	0.4932	0.3152	13.67

[b]*The number in bracket is the experimental value by Sada et al. [24].*

Table 3.
Dual-mode sorption parameters for carbon dioxide in polysulfone film as a function of operating temperature.

As for gas permeability of CO₂ through PSF membrane at varying pressures, it has been tabulated in **Figure 10**. Similarly, applicability of the data has been demonstrated through good compliance with published experimental data by Sada et al. [24].

It is found that gas permeability experiences a decrement before reaching the plasticization pressure at 34.9, 36.1 and 38.0 bars respectively for operating temperature of 35, 45 and 55°C. This has been attributed to rapid decrement in gas solubility when the sorption level off at high pressure due to saturation of favorable sites. Nevertheless, beyond the plasticization pressure, an increase in permeability has been observed because the diffusion coefficient increases with pressure much more rapidly than the solubility coefficient that decreases with pressure, which has been elucidated through plasticization effect that enhances the diffusivity of gas molecules to a large extend when the polymeric membrane is swelled. Viewing from the impact of plasticization pressure, it is shifted to higher value at greater operating temperature. This has been attributed to lower sorption of condensable CO₂ when the gas has the tendency to maintain at its gas state with increment in temperature.

The parameters for partial immobilization model of CO₂ have been summarized in **Table 4** with a similar trend observed to that for methane. Nonetheless, the parameters are only applicable to condition before the plasticization pressure is met. After that, the plasticization behavior has been characterized through Eq. (5) that describes permeability of gas within the glassy membrane undergoing plasticization [29].

$$P_i = \frac{D_{0,i}}{\beta_i f_i}\left[\exp\left(\beta_i k_{Di} f_i\left(1 + \frac{F_i C'_{Hi} b_i}{k_{Di}(1 + b_i f_i)}\right)\right) - 1\right] \tag{5}$$

Variables describing the modified partial immobilization model for plasticized membrane are provided in **Table 4** as well.

Regardless of demonstrating a similar trend of increment in value with increasing temperature, the $D_{0,i}$ values after plasticization are found to be relatively smaller as compared to its counterpart with pristine unaltered PSF structure. This has been attributed to a smaller amount of mobile gas when the favorable sites become concentrated and occupied. With respect to temperature dependency, β_i is found to decrease with increment in temperature, which implies that the plasticization potential reduces with temperature. It has been proposed that polymeric membrane experiences a decrement in Langmuir microvoids with increment in operating temperature [29]. Therefore, there are fewer pathways for CO₂ to interact with functional group of the polymeric chains, which consequently reduces the plasticization potential at higher temperature. In addition, the condensable CO₂ also has a higher tendency to exist in the gaseous state, which reduces its plasticization power when operating temperature is increased.
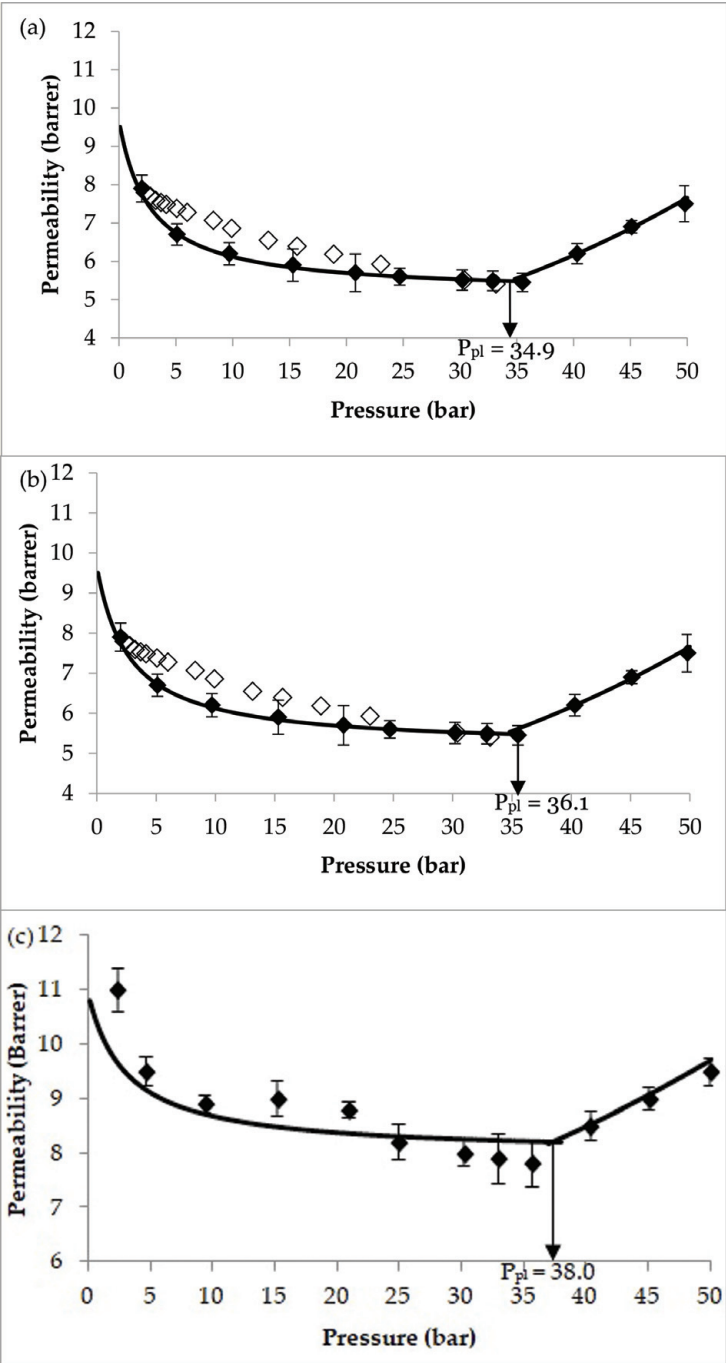
Figure 10.
*CO_2 gas permeability for polysulfone at (a) 35°C, (b) 45°C and (c) 55°C. [♦ In-house permeability data ◇ Permeability data by Sada et al. [24]. Line - Prediction of partial immobilization model by Eq. (4) and Eq. (5) with parameters in **Table 4** for in-house collected permeability].*

Temperature (°C)	$D_{0,i}$ ($\times 10^{-8}$ cm²/s)		F_i	β_i
	Before plasticization	After plasticization		
35	5.73	2.61	0.1307	0.0537
45	8.33	4.31	0.1107	0.0506
55	12.1	7.02	0.0856	0.0491

Table 4.
Partial immobilization parameters for CO_2 in polysulfone film as a function of operating temperature, model adapted from Scholes et al. [29].
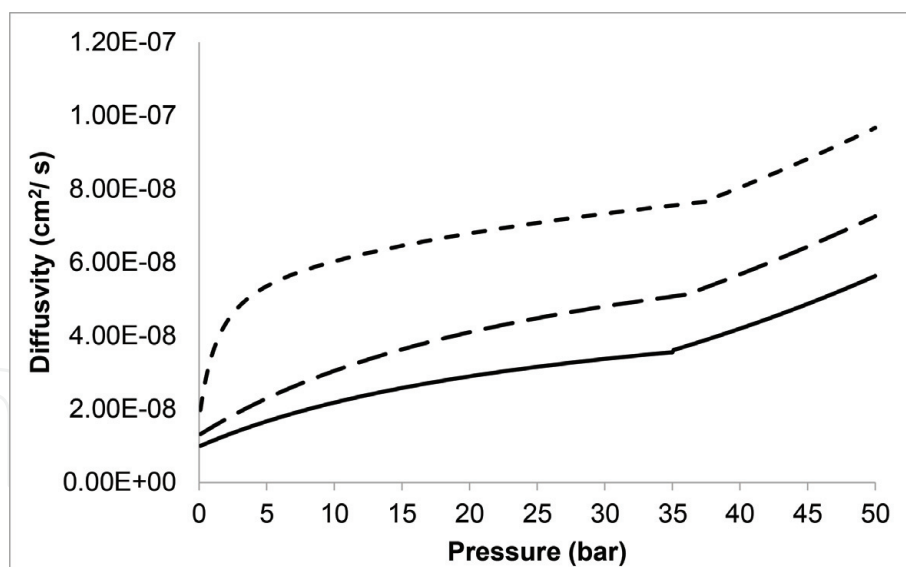
Figure 11.
CO$_2$ diffusivity for polysulfone (———— 35°C, ———— 45°C, ------- 55°C).

As for gas diffusivity shown in **Figure 11**, prior to CO$_2$ plasticization effect, the value at a low pressure is relatively lower, because most of the gas molecules are in the Langmuir mode and it has been reported that gas molecules sorbed into the Henry's mode sites inherit greater diffusivity than its counterpart [26].

The apparent diffusivity increases and reaches the asymptotic limit of diffusivity of Henry's Law proportion at high pressure. Nonetheless, it is found that after the plasticization pressure, gas diffusivity increases exponentially when pressure is further increased. The observation can be explained through enhanced interaction between CO$_2$ gas molecule and polymeric matrix, which contributes to augmented swelling and increment in free volume that forms pathway for diffusion of gas.

4. Conclusions

In present study, in house experimental work and setup has been conducted to fabricate, to characterize and to evaluate the gas transport properties in polysulfone (PSF) membrane film, typically those with plasticization characteristic. Validity of the solubility and gas permeability measurement has been demonstrated through good accordance with published experimental results and satisfactory empirical fitting to the dual mode sorption and partial immobilization models, which are well-known equations to quantify gas sorption and permeation in glassy polymeric membranes. To conclude, polysulfone membranes have permeability–pressure and concentration-pressure isotherms that vary with temperature. The plasticization potential decreases with temperature, implying that CO$_2$ ability to plasticize the polysulfone membrane reduces at higher temperature. In addition, the plasticization pressure is shifted to higher value with increment in temperature (34.9 bars at 35°C to 36.1 bars at 45°C to 38.0 bars at 55°C). In addition, gas permeability is found to be enhanced at greater operating temperature, which can be rationalized through greater activation energy to execute diffusional jump in increased free volume structure. From findings of present study, it is found that higher operating temperature is favorable for membrane operation since it promotes gas permeation, which enables more efficient removal of CO$_2$ from biogas under the same membrane area requirement. In addition, higher operating temperature also suppresses the effect of plasticization by exhibiting higher plasticization pressure. The study of CO$_2$

plasticization at varying operating temperatures is anticipated to be extended to mixed CO_2/CH_4 system to verify the behavior in real membrane gas separation.

Acknowledgements

Conflict of interest

The authors declare that there is no conflict of interest.

Author details

Serene Sow Mun Lock[1], Kok Keong Lau[1]*, Azmi Mohd Shariff[1], Yin Fong Yeong[1] and Norwahyu Jusoh[2]

1 CO_2 Research Center (CO_2RES), Department of Chemical Engineering, Universiti Teknologi PETRONAS, Seri Iskandar, Malaysia

2 Centre for Contaminant Control (CenCo), Department of Chemical Engineering, Universiti Teknologi PETRONAS, Seri Iskandar, Malaysia

*Address all correspondence to: laukokkeong@utp.edu.my

IntechOpen

References

[1] Song Z, Zhang C, Yang G, Feng Y, Ren G, Han X. Comparison of biogas development from households and medium and large-scale biogas plants in rural China. Renewable and Sustainable Energy Reviews. 2014;**33**:204-213. DOI: 10.1016/j.rser.2014.01.084

[2] Yépez-García RA, Dana J. Mitigating Vulnerability to High and Volatile Oil Prices: Power Sector Experience in Latin America and the Caribbean. Washington: The World Bank; 2012. DOI: 10.1596/978-0-8213-9577-6

[3] Hart A, Gnanendran N. Cryogenic CO$_2$ capture in natural gas. Energy Procedia. 2009;**1**:697-706. DOI: 10.1016/j.egypro.2009.01.092

[4] Hao J, Rice PA, Stern SA. Upgrading low-quality natural gas with H$_2$S- and CO$_2$-selective polymer membranes: Part I. Process design and economics of membrane stages without recycle streams. Journal of Membrane Science. 2002;**209**:177-206. DOI: 10.1016/S0376-7388(02)00318-6

[5] Gori G, Gabetta G. The use of knowledge management to improve pipeline safety. In: Bolzon G, Boukharouba T, Gabetta G, Elboujdaini M, Mellas M, editors. Integrity of Pipelines Transporting Hydrocarbons: Corrosion, Mechanisms, Control, and Management. Netherlands: Springer; 2010. pp. 1-16. DOI: 978-94-007-0588-3

[6] Marriott J, Sørensen E. A general approach to modelling membrane modules. Chemical Engineering Science. 2003;**58**:4975-4990. DOI: 10.1016/j.ces.2003.07.005

[7] Jung HJ, Han SH, Lee YM, Yeo Y-K. Modeling and simulation of hollow fiber CO$_2$ separation modules. Korean Journal of Chemical Engineering. 2011;**28**:1497-1504. DOI: 10.007/s11814-010-0530-y

[8] Coleman MR, Koros WJ. Conditioning of fluorine containing polyimides. 1. Effect of exposure to high pressure carbon dioxide on permeability. Macromolecules. 1997;**30**: 6899-6905. DOI: 10.1021/ma961323b

[9] Kikic I, Vecchione F, Alessi P, Cortesi A, Eva F, Elvassore N. Polymer plasticization using supercritical carbon dioxide: Experiment and modeling. Industrial & Engineering Chemistry Research. 2003;**42**:3022-3029. DOI: 10.1021/ie020961h

[10] Bos A, Pünt IGM, Wessling M, Strathmann H. CO$_2$-induced plasticization phenomena in glassy polymers. Journal of Membrane Science. 1999;**155**:67-78. DOI: 10.1016/S0376-7388(98)00299-3

[11] Wessling M, Schoeman S, van der Boomgaard T, Smolders CA. Plasticization of gas separation membranes. Gas Separation & Purification. 1991;**5**:222-228. DOI: 10.1016/0950-4214(91)80028-4

[12] Houde AY, Kulkarni SS, Kulkarni MG. Permeation and plasticization behavior of glassy polymers: A WAXD interpretation. Journal of Membrane Science. 1992;**71**:117-128. DOI: 10.1016/0376-7388(92)85011-7

[13] Kapantaidakis GC, Koops GH, Wessling M, Kaldis SP, Sakellaropoulos GP. CO$_2$ plasticization of polyethersulfone/polyimide gas-separation membranes. AIChE Journal. 2003;**49**:1702-1711. DOI: 10.002/aic.690490710

[14] Horn NR, Paul DR. Carbon dioxide plasticization and conditioning effects in thick vs. thin glassy polymer films. Polymer. 2011;**52**:1619-1627. DOI: 10.016/j.polymer.2011.02.007

[15] Tiwari RR, Smith ZP, Lin H, Freeman BD, Paul DR. Gas permeation in thin films of "high free-volume" glassy perfluoropolymers: Part II. CO_2 plasticization and sorption. Polymer. 2015;**61**:1-14. DOI: 0.1016/j.polymer. 2014.12.008

[16] Suleman MS, Lau KK, Yeong YF. Plasticization and swelling in polymeric membranes in CO_2 removal from natural gas. Chemical Engineering & Technology. 2016;**39**:1604-1616. DOI: 10.002/ceat.201500495

[17] Safari M, Ghanizadeh A, Montazer-Rahmati MM. Optimization of membrane-based CO_2-removal from natural gas using simple models considering both pressure and temperature effects. International Journal of Greenhouse Gas Control. 2009;**3**:3-10. DOI: 1016/j.ijggc.2008. 05.001

[18] Lock SSM, Lau KK, Shariff AM, Yeong YF, Bustam MA, Jusoh N, et al. An atomistic simulation towards elucidation of operating temperature effect in CO_2 swelling of polysulfone polymeric membranes. Journal of Natural Gas Science and Engineering. 2018;**57**:135-154. DOI: 10.1016/j. jngse.2018.07.002

[19] Wijenayake SN, Panapitiya NP, Versteeg SH, Nguyen CN, Goel S, Balkus KJ, et al. Surface cross-linking of ZIF-8/polyimide mixed matrix membranes (MMMs) for gas separation. Industrial & Engineering Chemistry. 2013;**52**:6991-7001. DOI: 10.1021/ ie400149e

[20] Jusoh N, Yeong YF, Lau KK, Shariff MA. Enhanced gas separation performance using mixed matrix membranes containing zeolite T and 6FDA-durene polyimide. Journal of Membrane Science. 2017;**525**:175-186. DOI: 10.1016/j.memsci.2016.10.044

[21] Stern SA, De Meringo AH. Solubility of carbon dioxide in cellulose acetate at elevated pressures. Journal of Polymer Science Part B: Polymer Physics. 1978; **16**:735-751. DOI: 10.1002/pol.978. 180160415

[22] Huang Y, Paul DR. Effect of film thickness on the gas-permeation characteristics of glassy polymer membranes. Industrial & Engineering Chemistry. 2007;**46**:2342-2347. DOI: 10.1021/ie0610804

[23] Struik LCE. Physical aging in amorphous glassy polymers. Annals of the New York Academy of Sciences. 1976;**279**:78-85. DOI: 10.1111/ j.749-6632.1976.tb39695.x

[24] Sada E, Kumazawa H, Xu P, Nishigaki M. Mechanism of gas permeation through glassy polymer films. Journal of Membrane Science. 1988;**37**:165-179. DOI: 10.1016/ S0376-7388(00)83070-7

[25] Barrer RM, Barrie JA, Slater J. Sorption and diffusion in ethyl cellulose. Part III. Comparison between ethyl cellulose and rubber. Journal of Polymer Science. 1958;**27**:177-197. DOI: 10.1002/ pol.958.1202711515

[26] Koros WJ, Paul DR, Rocha AA. Carbon dioxide sorption and transport in polycarbonate. Journal of Polymer Science. 1976;**14**:687-702. DOI: 10.1002/ pol.976.180140410

[27] Lock SSM, Lau KK, Shariff AM, Yeong YF, Bustam MA. Thickness dependent penetrant gas transport properties and separation performance within ultrathin polysulfone membrane: Insights from atomistic molecular simulation. Journal of Polymer Science Part B: Polymer Physics. 2018;**56**: 131-158. DOI: 10.1002/polb.24523

[28] Story BJ, Koros WJ. Comparison of three models for permeation of

CO$_2$/CH$_4$ mixtures in poly(phenylene oxide). Journal of Polymer Science. 1989;**27**:1927-1948. DOI: 10.002/polb.89.090270910

[29] Scholes CA, Chen GQ, Stevens GW, Kentish SE. Plasticization of ultra-thin polysulfone membranes by carbon dioxide. Journal of Membrane Science. 2010;**346**:208-214. DOI: 10.1016/j.memsci.2009.09.036